

Hyaluronic acid stimulates the formation of calcium phosphate on CoCrMo alloy in simulated physiological solution

Ingrid Milošev · Julija Hmeljak · Andrej Cör

Received: 24 July 2012 / Accepted: 30 November 2012 / Published online: 19 December 2012
© Springer Science+Business Media New York 2012

Abstract The behaviour of CoCrMo alloy has been studied in two simulated physiological solutions—NaCl and Hanks' solutions—each containing the sodium salt of hyaluronic acid. Hyaluronic acid is a component of synovial joint fluid, so the behaviour of orthopaedic alloys in its presence needs to be assessed. Electrochemical methods, X-ray photoelectron spectroscopy and scanning electron microscopy have been used to analyse the composition, thickness and morphology of any layers formed on the alloy. The addition of hyaluronic acid shifts the corrosion potential and increases the value of polarization resistance. The presence of hyaluronic acid in simulated Hanks' physiological solution stimulates the formation of a calcium phosphate layer, opening up the possibility for tailoring the surface properties of CoCrMo alloy. The viability of human osteoblast-like was determined using the Alamar[®] Blue Assay, while the osteogenic activity was evaluated by alkaline phosphatase activity. The presence of hyaluronic acid affects the alkaline phosphatase activity.

1 Introduction

Prolongation of their life-time is the main goal of research studies on implant materials. In addition to macro-factors like implant design and surgical techniques, successful implantation is based on the formation of a thin (0.1–1 nm) implant/bone interface layer [1]. Modifications of the surface of metallic biomaterials to establish a stable interface layer and a desirable biological response can be divided into physicochemical, morphological and biochemical approaches [2, 3]. Physicochemical methods are aimed at altering surface energy, charge and composition, such as the formation of calcium phosphate coatings [4]. Morphological methods comprise alterations in morphology and roughness, while biochemical approaches are directed at controlling cell adhesion.

Although much is already known about surface modification and interface formation, many questions remain unresolved, especially regarding the relationships between composition of the bio-environment and the mechanical, structural and chemical properties of the metal surface. In vitro corrosion studies on CoCrMo alloy, one of the most important alloys used in orthopaedics, have mostly been carried out in simple solutions of inorganic salts [5–8], as recently reviewed [9]. The passivity of CoCrMo alloy is due to the formation predominantly of Cr₂O₃ and Cr(OH)₃, followed by the formation of CoO and MoO₃ at more positive electrode potentials [9]. However, studies in inorganic simulated physiological solutions must be regarded as initial attempts only to understand the in vivo behaviour of a metal. Conditions in the human body can be mimicked more closely by performing experiments in cell culture media and in the presence of serum or cells [10–12]. For titanium, a correlation between calcium and phosphorus ions and proteins has been reported; both

I. Milošev (✉)
Department of Physical and Organic Chemistry, Jožef Stefan
Institute, Jamova c. 39, 1000 Ljubljana, Slovenia
e-mail: ingrid.milosev@ijs.si

I. Milošev · A. Cör
Valdoltra Orthopaedic Hospital, Jadranska c. 31,
6280 Ankaran, Slovenia

J. Hmeljak · A. Cör
Faculty of Health Sciences, University of Primorska,
Polje 42, 6310 Izola, Slovenia

calcium phosphate deposition and protein adsorption decreased the cathodic current [13]. We have recently studied the influence of the composition of a simulated physiological solution on the surface layers formed on a CoCrMo alloy in order to determine the effect of particular inorganic and organic components [14]. Special emphasis was given to the effect of synovial fluid which forms part of the natural environment of a metal joint prosthesis. In the simulated Hanks' physiological solution containing synovial fluid less calcium phosphate is formed and the formation of metal oxide was hindered [14]. Similar results were published by Yadav and Brown [15]. The formation of stoichiometric hydroxyapatite occurred more rapidly in simulated Hanks' solution and distilled water than in serum. The latter strongly inhibits hydroxyapatite formation.

In the present investigation the simulated physiological solution was enriched with hyaluronic acid (HA), an important component of synovial fluid. HA regulates many important physiological and pathophysiological reactions. It is a glycosaminoglycan (GAG) or mucopolysaccharide, a long, unbranched polysaccharide composed of repeating units of disaccharides. HA is periodic structure of disaccharide *N*-acetyl-*D*-glucosamine and *D*-glucuronic acid [16]—the only non-sulfated GAG and a high molecular mass polymer in excess of 10^6 Da. It is present in connective, epithelial and neural tissues and is one of the main components of the extracellular matrix of cartilage. It affects cell proliferation and migration and is responsible for the viscosity and resistance to compressive stress of synovial fluid. HA, as the main component of skin dermis extracellular matrix, is involved in skin healing and is commonly found in skin care products. HA is popularity also used as scaffold in tissue engineering, as well as for treatment of pain with knee osteoarthritis [17].

At physiological pH and ionic strength HA in solution is described as stiffened random coil. The rigidity is related to the intramolecular hydrogen bonds between glycoside groups and the electrostatic repulsion between carboxyl groups [18]. In solution, electrostatically induced contraction can occur and the HA conformation thus depends on the composition and pH of the electrolyte. In the presence of Na^+ ions a fourfold helix is formed [19], and a threefold helix in the presence of Ca^{2+} ions. Calcium ions play an important role in the type of HA conformation and consequently its mechanical properties, i.e. flexibility of the related matrix [18, 19]. Gribbon et al. [18] suggested that the effects of electrolytes and solvents are determined primarily by their effect on HA chain flexibility. Calcium ions increase the chain flexibility (promote chain contraction) by promoting a greater range of movement at each glycosidic bond. A similar effect was observed for Mn^{2+} , but much less so for Na^+ and K^+ [18, 19]. Calcium ions can act as bridge between a TiO_2 surface and HA.

Adsorption of proteins probably proceeds in similar manner [20, 21]. The affinity of titanium for calcium ions is the basis for the spontaneous formation of calcium phosphate and its ability to integrate with bone [22].

The aim of the present study was to investigate the effect of hyaluronic acid on the behaviour of the CoCrMo alloy, especially in terms of interaction with inorganic salts present in simulated physiological solution.

2 Experimental

2.1 Material

The CoCrMo alloy used in this work is that used for the manufacture of the femoral head of hip prostheses produced by the company Zimmer. Its composition complies with the International Standard Organization (ISO) standard ISO 5832-12:2007(E) "Implants for surgery—Metallic materials—Part 12—Wrought cobalt–chromium–molybdenum alloy". The test specimens were in the form of discs 15 mm in diameter and 2 mm thick. The samples were ground mechanically under water with SiC papers successively from 320 up to 4.000 grit, followed by cleaning with ethanol in an ultrasonic bath for two minutes, double-rinsing with Milli-Q water, and finally drying in a stream of nitrogen.

2.2 Electrochemical measurements

Electrochemical measurements were performed in a conventional three-electrode cell (volume 300 mL) at a temperature of 37 ± 1 °C. The working electrode was embedded in a Teflon holder, with an area of 0.785 cm^2 exposed to the solution. The counter-electrode was graphite. Potentials were measured against a saturated calomel electrode (SCE) connected to the cell via a Luggin probe. Measurements were carried out with an Autolab PGSTAT 12 potentiostat/galvanostat (Metrohm Autolab, Utrecht, The Netherlands) controlled by Nova 1.8. Prior to measurement, samples were allowed to stabilize under open conditions for various times of immersion (up to 24 h) to reach a stable value of the corrosion potential, E_{corr} . Linear polarization measurements were then made at 0.1 mV/s scan rate in the range $\pm 10 \text{ mV}$ versus E_{corr} , followed by potentiodynamic measurements at 1 mV/s scan rate, starting at E_{corr} and increasing in the anodic direction. For each solution, measurements were performed at least in duplicate. Mean values and standard deviations were determined. For graphical presentation in the form of potentiodynamic polarization curve a representative measurement was chosen. Electrochemical measurements were performed in the following solutions:

1. 0.9 % NaCl (denoted as NaCl). The pH was adjusted to pH 7.4 by addition of HCl or NaOH (1 M) solution.
2. Hanks' simulated physiological solution (denoted as HS) with the following composition: 8 g/L NaCl, 0.4 g/L KCl, 0.25 g/L $\text{NaH}_2\text{PO}_4 \cdot 2\text{H}_2\text{O}$, 0.35 g/L NaHCO_3 , 0.06 g/L $\text{Na}_2\text{HPO}_4 \cdot 2\text{H}_2\text{O}$, 0.19 g/L $\text{CaCl}_2 \cdot 2\text{H}_2\text{O}$, 0.4 g/L $\text{MgCl}_2 \cdot 6\text{H}_2\text{O}$, 0.06 g/L $\text{MgSO}_4 \cdot 7\text{H}_2\text{O}$, and 1 g/L glucose. The pH was adjusted to 7.4 by addition of HCl or NaOH (1 M) solution.

All chemicals were of *p.a.* purity, and used as received from Applichem GmbH, Germany, Fluka, Germany, Sigma-Aldrich, Germany, or Sigma Life Science, USA. Solutions were prepared using Milli-Q Direct water (Millipore, Billerica, MA) with a resistivity of 18.2 M Ω cm at 25 °C.

Sodium salt of hyaluronic acid was added, where stated, at a concentration range from 1 to 4 g/L. It was supplied by Calbiochem (Merck KGaA, Darmstadt, Germany) and used as received.

2.3 X-ray photoelectron spectroscopy (XPS) and scanning electron microscopy (SEM)

XPS was performed with a TFA Physical Electronics Inc. spectrometer, using non- and mono-chromatized Al K_{α} radiation (1486.6 eV) and a hemispherical analyser [14]. Angle-resolved XPS (AR-XPS) measurements were conducted at take-off angles of 20°, 45° and 80° with respect to the surface plane to obtain depth-dependent information on the composition and structure of the layers. The depth analysed increases with increased angle, in practice up to 10 nm [23]. Thus at small angles (20°) information is provided closer to the surface and, at large angles (80°), closer to the bulk. The procedures of XPS analysis were as described [8, 14]. The centre of the $2p_{3/2}$ peak for Cr metal is situated at 574.2 eV and shifted to 576.3 and 577.5 eV with the formation of Cr_2O_3 and $\text{Cr}(\text{OH})_3$, respectively. In a Cr(VI) compound the $2p_{3/2}$ peak is situated at 578.7 eV. The centre of the Co $2p_{3/2}$ peak in Co metal is located at 778.1 eV, and is shifted to 780.5–781.2 eV by cobalt oxides (mixed CoO , Co_2O_3 and Co_3O_4). The centre of the Mo $3d_{5/2}$ peak in Mo metal is at 227.6 eV, and at 232.1–232.5 eV for MoO_3 .

The following reference positions of the oxygen species were considered in the O 1s peak: oxide (O^{2-}) at 530.1–530.3 eV, hydroxide (OH^-) at 531.4–531.6 eV, water (H_2O) and/or phosphate (PO_4^{3-}) at 532.3–532.5 eV, and organic oxygen species (O_{org}) at 533.4–533.6 eV. The following reference positions of the carbon species were considered in the C 1s peak: aliphatic carbon (C–C, C–H) at 284.8–285.0 eV, carbon bonded to oxygen (C–O) at 286.0–286.2 eV, and carbon bonded to nitrogen in organic compounds (C_{org}) at 287.0–288.0 eV. The nitrogen in

organic compounds is registered in the N 1s peak located at 400.4–400.6 eV and denoted as N_{org} .

After recording the spectra at the layer surface, depth profiles of the oxidized layers were determined using an Ar^+ ion beam with an energy level of 1 keV and a raster of 3 mm \times 3 mm. Sputter rate was determined on the SiO_2 standard supplied by RBD Instruments (<http://www.rbdinstruments.com>) according to [24].

The morphology of the surface layers was analysed using a field emission scanning electron microscope (FE-SEM) Ultra+ (Carl Zeiss). Images were recorded using low accelerating voltages of 0.2 and 1 kV, with no sample preparation.

2.4 Cell culture

Human osteosarcoma (HOS) cells from a human osteoblast-like cell line (ATCC no. CRL-1543) were used for ex vivo biocompatibility testing. They were cultured routinely in Advanced[®] MEM, supplemented with 5 vol% foetal bovine serum and 15 $\mu\text{g}/\text{mL}$ gentamicin (all Gibco, Carlsbad, CA, USA), at 37 °C in a humidified atmosphere with 5 vol% CO_2 .

All solutions for alloy immersion experiments were sterile filtered using a membrane filter with 0.2 μm pores (Sartorius, Göttingen, Germany) and refrigerated until use. Effects on viability and alkaline phosphatase activity were determined after exposing cells to a mixture of 1/3 test solution and 2/3 of complete growth medium.

All cell-based experiments were performed in triplicate. HOS cells grown in 2/3 complete growth medium and 1/3 phosphate buffered saline (PBS) were used as negative (unexposed) controls. Statistical analyses were performed with SigmaPlot 11.0 (Systat Software, Chicago, IL, USA). Student's t test was used for comparisons between treatment groups and statistical significance was set at $P < 0.05$ for all tests.

2.5 Cell viability

Cell viability was assessed using the fluorimetric Alamar Blue[®] assay (Invitrogen, Carlsbad, CA, USA). Five hundred cells were seeded in each well of a black, flat bottomed 96-well cell culture plate (Greiner, Frickenhausen, Germany). Cells were incubated in a mixture of complete growth medium (60 μL) and test solution (30 μL) for 3 days. On the 4th day, 10 μL of Alamar Blue reagent was added to each well and the plates further incubated for 2 h at 37 °C before measuring fluorescence at 535 nm using an Infinite 200 microplate reader (Tecan, Männedorf, Switzerland).

Fluorescence measurements were corrected by subtracting the average value of the blank (cell-free) measurements.

Relative cell viability was expressed as the ratio of fluorescence generated by exposed to test solutions to that of cells exposed to Hanks' simulated physiological solution only.

2.6 Alkaline phosphatase (ALP) activity

5×10^4 cells were seeded in each well of a 6-well clear cell culture plate (Greiner) in a mixture of 300 μL test solution and 600 μL complete growth medium. Negative (unexposed) controls were grown in either 900 μL of complete growth medium or a mixture of 300 μL PBS and 600 μL complete growth medium.

Cells were incubated for three days. On the 4th day, cells were harvested, counted and aliquots of 1×10^5 cells prepared for ALP activity measurement.

Differences in ALP activity between exposed cells and unexposed controls were assessed using the fluorometric Alkaline Phosphatase Assay Kit (Abcam, Cambridge, UK) according to the manufacturer's protocol. 1×10^5 cells were lysed in 110 μL of Assay Buffer and centrifuged. Supernatants were transferred into the wells of a black, flat bottomed 96-well cell culture plate (Greiner) and 20 μL of ALP substrate methylumbelliferyl phosphate disodium salt (MUP) added to each well. Plates were incubated in the dark at room temperature for 30 min. After incubation, the reactions were stopped by adding 20 μL of Stop Solution to each well and fluorescence at 360 nm was measured using a GENios microplate reader (Tecan).

Control values of fluorescence were obtained as above, using unexposed cells and stopping the reaction immediately after addition of MUP. ALP activity was obtained by subtracting the average fluorescence of background control from the average fluorescence of each experiment. ALP activity was obtained using a calibration curve (pure ALP enzyme supplied in the kit) and expressed as nmol 4-MU generated during the assay.

3 Results and discussion

3.1 Electrochemical measurements

The effect of the time, t_{imm} , of immersion of CoCrMo alloy at the open circuit potential, E_{oc} , was studied in 0.9 % NaCl (NaCl) and simulated Hanks' physiological solution (HS), with and without the addition of 4 g/L hyaluronic acid (HA). In NaCl alone, E_{oc} initially shifted to more negative values but, after ~ 500 s, moved to more positive values due to passive film formation. In HS, the E_{oc} shifted to more positive values immediately after immersion. The corrosion potential, E_{corr} , is defined as the E_{oc} value at the end of the immersion period. E_{corr} values were measured

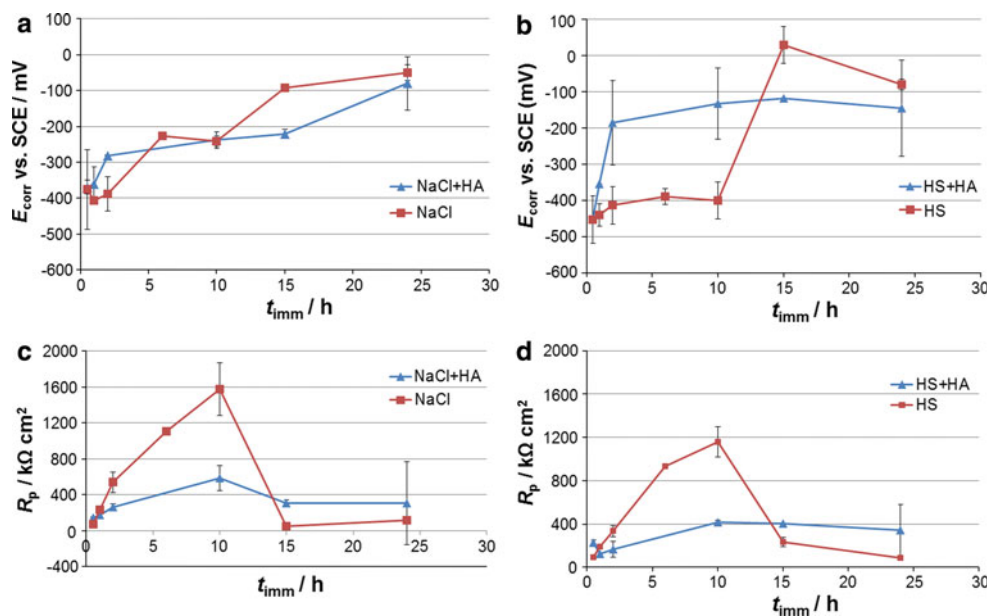
following different times of immersion in NaCl and HS (Fig. 1a, b). With increasing t_{imm} the values of E_{corr} shifted to more positive values, reflecting the formation and growth of a passive film of CoCrMo alloy. The shift was steeper in NaCl than in HS, in which the value of E_{corr} did not change significantly up to 10 h immersion but then shifted to more positive values. After 24 h, the values of E_{corr} are similar in the two solutions: -0.050 V in NaCl and -0.079 V in HS.

The addition of HA to NaCl did not change significantly the values of E_{corr} (Fig. 1a) which followed a trend similar to that in NaCl alone. In HS containing HA, the values of E_{corr} increased progressively with time (Fig. 1b). After 24 h immersion, the values were more negative than in plain HS, as observed in NaCl.

Polarization resistance, R_p , was measured following stabilization at the E_{oc} (Fig. 1c, d). In solutions with and without HA values of R_p increased with increasing t_{imm} and, after 10 h, exceeded $1 \text{ M}\Omega \text{ cm}^2$, indicating that the layer had become highly protective. After 10 h the values of R_p decreased considerably and, after 24 h, reached similar values in the two solutions: $118 \text{ k}\Omega \text{ cm}^2$ in NaCl and $85 \text{ k}\Omega \text{ cm}^2$ in HS. As will be seen below, the layer thickness and composition does not change much with increasing immersion time. Therefore, it is reasonable to assume that this decrease in R_p is related to a change in the course of the corrosion process at the surface, and, consequently, to a change in the electronic properties of the layer.

The surface layer formed on Ti-based alloy in simulated physiological solution has been described by a two-layer model that comprises an inner, barrier layer that is largely responsible for the high corrosion resistance, and an outer, porous layer [25–29]. A similar model has been used to describe the surface layer formed on CoCrMo alloy in simulated physiological solution [30]. Such changes of resistance of the layer during immersion in simulated physiological solution have been reported. After an initial increase, the R_p values decreased after 10 h immersion of the Ti-6Al-7Nb alloy in simulated physiological solution [31]; at the same time the R_p values increased continuously. It was assumed that, in the initial immersion period, the oxide layer thickens and its resistance increases, but then some cracks or defects appear, leading to re-activation of the corrosion process and decrease in the resistance. Afterwards a steady-state is established with similar R_p values in both solutions. Souto et al. [27] observed a drop in R_p after 12 days of immersion; after which stationary conditions were observed up to 125 days. In the presence of HA no pronounced maximum was observed, as for plain NaCl and HS solutions (Fig. 1c, d). Instead, the values increased with increasing immersion time and after 24 h were seven and sixfold higher than in plain NaCl and HS

Fig. 1 **a, b** Corrosion potential, E_{corr} , and **c, d** polarization resistance, R_p , recorded for CoCrMo alloy as a function of time of immersion, t_{imm} , in 0.9 % NaCl and simulated Hanks' physiological solution (HS), with and without addition of 4 g/L hyaluronic acid (HA). Data are mean values (symbol) \pm SD (bars)



solutions. This indicates that, in the presence of HA, a surface layer with increased corrosion resistance is formed.

The immersion time at the E_{oc} has a decisive effect on the shape of the potentiodynamic polarization curves recorded in NaCl and HS (Fig. 2). The values of starting potential, E_{corr} , are gradually shifted in a positive direction and the current density decreases. This behaviour was noted previously in buffered 0.14 M NaCl and ascribed to passive film growth, to a change in composition or to a change in a passive film structure [6]. The addition of 4 g/L HA causes an additional shift of E_{corr} to more positive values (Fig. 2). This shift is more pronounced in HS than in NaCl, and is greatest after 10 h immersion, when it decreases (Fig. 1). Due to the shift of E_{corr} the shape of the polarization curves in HS is also affected by the t_{imm} . Unlike the plain solution, it reaches the passive region in the second half of its span and then continues virtually without change. The transpassive range is not affected by the presence of HA or by the time of immersion.

The effect of HA concentration was studied at 1, 2 and 4 g/L for a constant immersion time of 1.5 h at the E_{oc} (Table 1). While, in NaCl, the E_{corr} shifted to somewhat more negative values with increasing HA concentration, in HS it shifted to significantly more positive values (by +150 mV). However, despite the difference in the trend of E_{corr} in the two solutions, the values of polarization resistance changed only slightly with increasing HA concentration and reached similar values in both solutions.

These data indicate that (i) CoCrMo alloy behaves differently in NaCl and HS, and (ii) the addition of HA has a decisive effect on the behaviour of this alloy, especially in HS. Based on the electrochemical results presented the study was concentrated on the effect on the addition of two

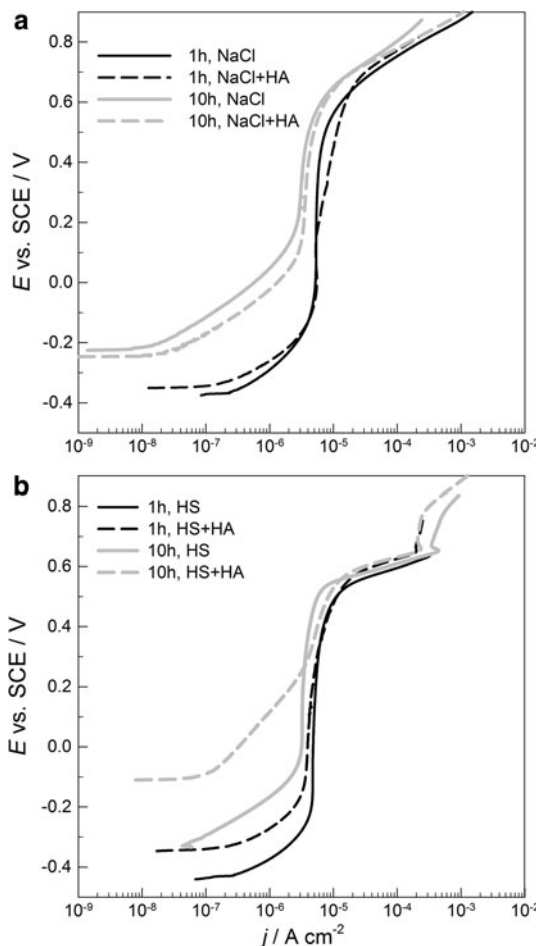


Fig. 2 Potentiodynamic polarization curves recorded for CoCrMo alloy in **a** 0.9 % NaCl and **b** in simulated Hanks' physiological solution (HS) with and without addition of 4 g/L hyaluronic acid (HA) after 1 and 10 h immersion time at the open circuit potential, E_{oc}

Table 1 Values of corrosion potential, E_{corr} , and polarization resistance, R_p , measured for CoCrMo alloy after 1.5 h immersion in 0.9 % NaCl and simulated Hanks' physiological solution (HS) containing various concentrations of hyaluronic acid (HA)

HA concentration (g/L)	Simulated physiological solution			
	NaCl		HS	
	E_{corr}/V	$R_p/k\Omega \text{ cm}^2$	E_{corr}/V	$R_p/k\Omega \text{ cm}^2$
0	-0.310 ± 0.038	382 ± 133	-0.311 ± 0.054	412 ± 182
1	-0.302 ± 0.005	220 ± 14	-0.284 ± 0.032	243 ± 9
2	-0.358 ± 0.023	297 ± 25	-0.189 ± 0.003	255 ± 14
4	-0.323 ± 0.016	233 ± 28	-0.161 ± 0.045	262 ± 32

Data are given as mean value \pm SD

concentrations of HA (1 and 4 g/L) and two immersion times (1 and 15 h) at the E_{oc} in NaCl and HS. The samples were analysed by X-ray photoelectron spectroscopy (XPS) to provide the general chemical composition of the layers, the oxidation states of particular elements, as deduced from high resolution spectra, the structure of the sub-surface layers obtained by angle resolved spectra, and in-depth composition and thickness of the layers obtained by depth profiling. The morphology of the layers was investigated by field-emission scanning electron microscopy (FE-SEM).

3.2 Chemical composition and thickness of the layers formed in NaCl and simulated Hanks' physiological solution

The compositions of surface layers formed in plain NaCl and HS over 15 h immersion were deduced from XPS survey spectra (Table 2). The surfaces contained a high level of carbon, due to exposure to air. The high concentrations of oxygen and chromium are in accordance with the prevalent formation of chromium oxide [5–10, 14, 30]. The concentration of chromium is higher in NaCl than in HS. Compared to chromium, the surface layers formed in NaCl and HS contain approximately four and twofold, lower concentrations of cobalt. The concentration of molybdenum in the surface layer is even lower, less than 1 at. %. The significant difference between the NaCl and HS solution is the presence of calcium and phosphorus at the surface layer formed in HS, which is clearly related to the formation of calcium phosphate in this solution. The ratio Ca/P is 0.76, approximately twofold smaller than in hydroxyapatite (Ca/P = 1.67).

Normalized XPS Cr 2p spectra recorded at the surfaces of samples previously immersed in NaCl and HS are presented in Fig. 3a. Deconvolution of metal peaks has been presented in detail [8, 14]. The centre of the peak is located at 577.5 eV, consistent with the formation of chromium oxide/hydroxide. The peak related to chromium metal at 574.2 eV is still visible but much smaller than the oxide/hydroxide peak. A different situation is encountered in

Table 2 Composition of layers formed on CoCrMo alloy after 15 h immersion in 0.9 % NaCl and simulated Hanks' physiological solution (HS) with and without addition of 1 and 4 g/L hyaluronic acid (HA).

Element	Concentration/at. %					
	NaCl			HS		
	0 g/L HA	1 g/L HA	4 g/L HA	0 g/L HA	1 g/L HA	4 g/L HA
O 1s	44.1	43.8	42.7	51.4	50.8	50.8
C 1s	37.9	41.3	40.2	26.9	23.2	23.4
Cr 2p	13.9	8.1	6.2	10.5	0.7	1.0
Co 2p	3.6	2.2	1.7	4.4	1.0	–
Mo 3d	0.5	0.8	0.6	0.8	–	–
N 1s	–	3.8	5.1	–	1.5	3.5
Mg 2s	–	–	–	–	2.5	1.0
Na 1s	–	–	1.9	–	–	–
P 2p	–	–	1.6	3.4	9.4	9.4
Ca 2p	–	–	–	2.6	10.9	10.9
Ca/P	–	–	–	0.76	1.16	1.16

Composition was deduced from XPS survey spectra

cobalt Co 2p and molybdenum Mo 3d spectra (Fig. 3b, c). For these elements the peak centre is located in the metal range, i.e. at 778.1 eV for the Co 2p_{3/2} peak, and at 227.6 eV for the Mo 3d_{5/2} peak. Therefore, the formation of the related oxides is much less than that of chromium oxide, where the peak centre is located in the oxide range. Chromium oxide is thus the major component of the passive layer formed spontaneously at the surface of the CoCrMo alloy after immersion at the E_{oc} in NaCl and HS. The centre of the oxygen O 1s peak (Fig. 4a) is located at 531.9 eV in NaCl and 531.5 eV in HS, consistent with the formation of oxide and hydroxide layers, respectively. The centre of the carbon C 1s peak at 285.0 eV (Fig. 4b) confirming the presence of aliphatic carbon and is related to the exposure of samples to air between preparation and XPS analysis.

Besides oxides, the surface layer formed in HS contains calcium phosphate, as evidenced by the calcium Ca 2p and phosphorus P 2p spectra (Fig. 5). The position of Ca 2p is at 347.7 eV (Fig. 5a), in agreement with the position of peaks of $\text{Ca}_8\text{H}_2(\text{PO}_4)_6 \cdot 5\text{H}_2\text{O}$ at 347.2 eV, CaHPO_4 at 347.6 eV, and $\text{Ca}_{10}(\text{PO}_4)_6(\text{OH})_2$ at 347.8 eV [32]. The peak related to phosphorus, P 2p, appears at 133.6 eV (Fig. 5b) and can be related to the following compounds: $\text{Ca}_3(\text{PO}_4)_2$ at 132.9 eV, CaHPO_4 at 133.8 eV, and CrPO_4 at 133.4 eV [32]. Calcium and phosphorus are present in Hanks' solution as inorganic salts (see Experimental). Once dissolved in solution, these ions tend to form a variety of calcium phosphates, due to preferential adsorption of phosphate ions [33]. Phosphate ions are adsorbed by a hydrated titanium oxide surface during the release of protons, and calcium ions are adsorbed by phosphate ions. Eventually, calcium phosphate is formed. The presence of phosphate is important for the protective ability and reactivity of metals [33]. The titanium phosphate formed in titanium in Ca-free solution is not protective, while calcium phosphate formed on Ti is stable and protective [33]. Comparison of immersion in a Hanks' solution and in a solution containing phosphates or only Ca-ions, shows that

the presence of phosphate is necessary for the adsorption of Ca-ions, since the initial layer adsorbed on the Ti surface is phosphate [34]. The layer of phosphate therefore acts as a precursor to induce the nucleation of calcium phosphate. Calcium phosphate formation was also observed on CoCrMo alloy [10]; however, the Ca/P ratios were smaller than those on titanium. The layer formed after 7-days immersion of the CoCrMo alloy contained calcium phosphate with Ca/P ratios of 0.7 [10], similar to the value of 0.76 obtained in the present work.

Depth profiles of the surface layers formed in NaCl and HS during 15 h immersion are presented in Figs. 6a and 7a. The concentration of carbon decreased shortly after the sputter process began, indicating that it is a surface contaminant. The surface concentration of oxygen amounts to 40–50 at.%. It decreased with sputtering time, while the contents of Co, Cr and Mo increased. In HS the concentrations of Ca and P are below 4 at.% (Table 2; Fig. 7a, inset). The time at which the concentration of oxygen drops to half the surface concentration is used to estimate the layer thickness. The thickness: 4.6 nm in NaCl and 3.6 nm in HS, is similar in the two solutions. It is interesting that in HS the surface layer is somewhat thinner, despite

Fig. 3 Normalized XPS **a** Cr 2p, **b** Co 2p_{3/2}, and **c** Mo 3d spectra recorded at the layer formed on CoCrMo alloy after 15 h immersion in 0.9 % NaCl and Hanks' simulated physiological solution (HS) with and without addition of 1 and 4 g/L hyaluronic acid (HA). Dashed lines denote the positions of (a) (1) Cr (2) $\text{Cr}(\text{OH})_3$ (3) CrO_3 (b) (1) Co (2) $\text{CoO}/\text{Co}_2\text{O}_3/\text{Co}_3\text{O}_4$, and (c) (1) Mo (2) MoO_3

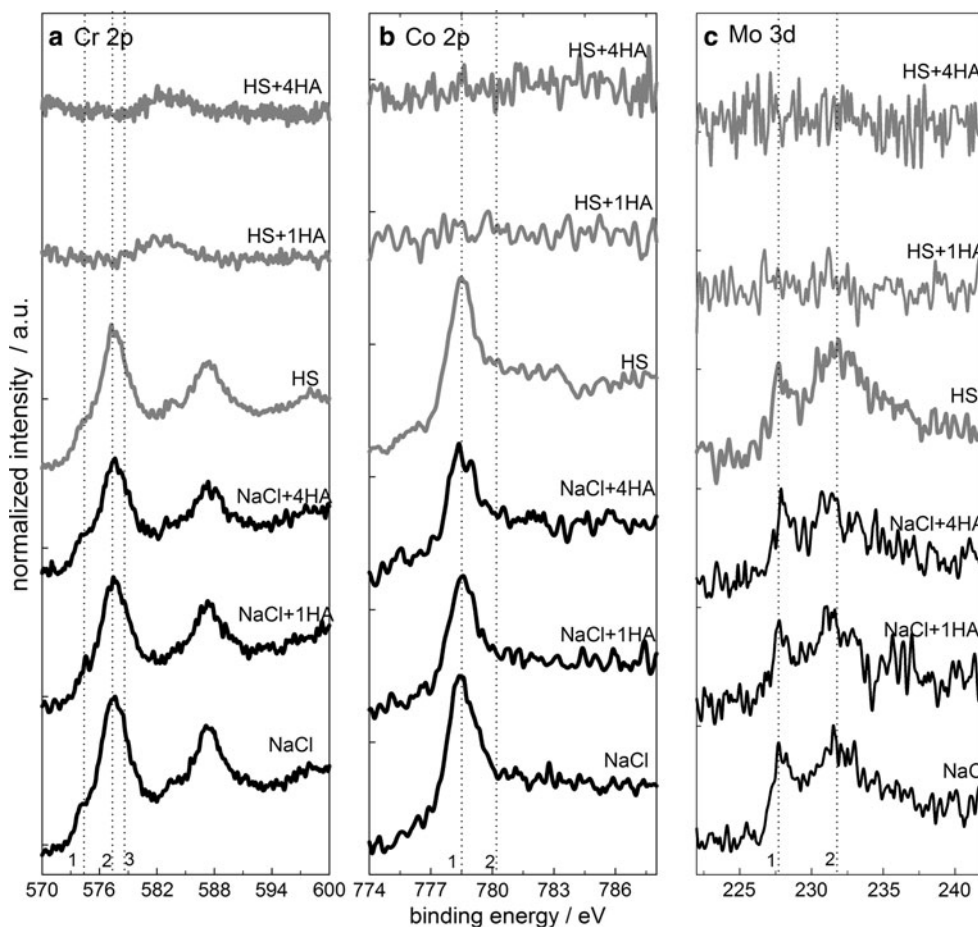
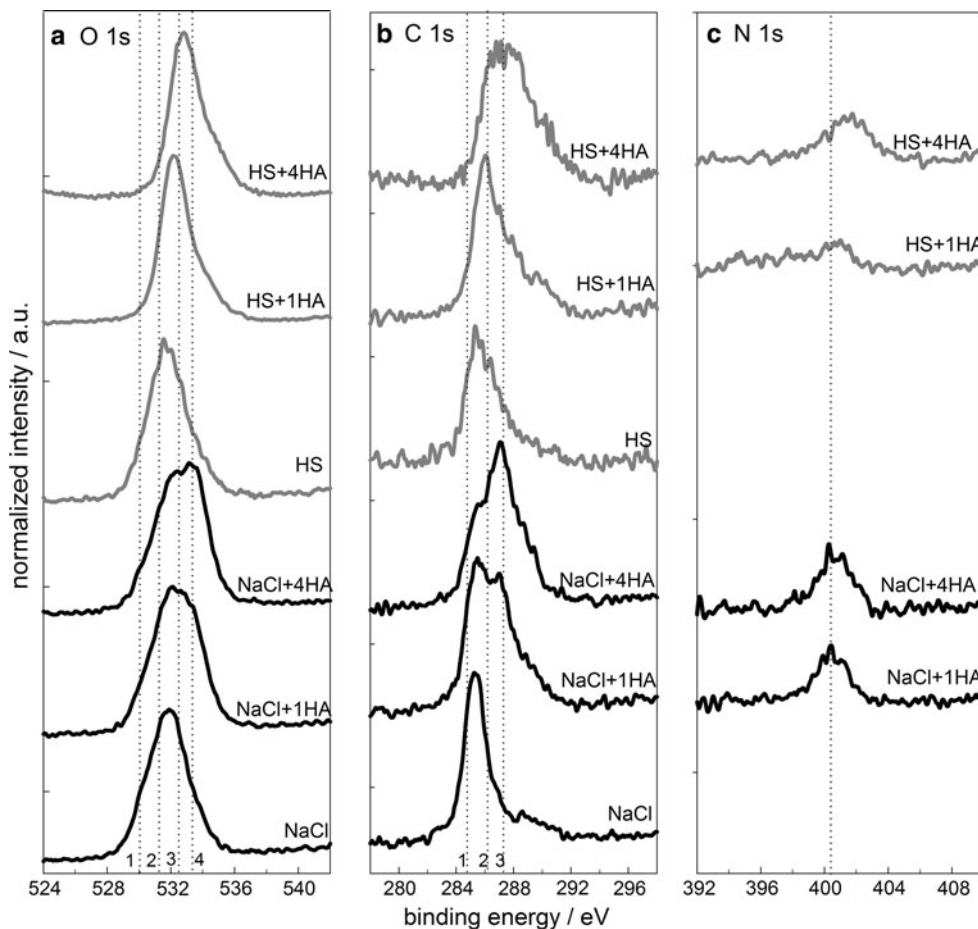


Fig. 4 Normalized XPS **a** O 1s **b** C 1s, and **c** N 1s spectra recorded at the layer formed on CoCrMo alloy after 15 h immersion in 0.9 % NaCl and Hanks' simulated physiological solution (HS) with and without addition of and 4 g/L hyaluronic acid (HA). Dashed lines denote the positions of (a) (1) O^{2-} (2) OH^- (3) PO_4^{3-} (4) O_{org} (b) (1) C–C, C–H (2) C–O (3) C_{org} , and (c) N_{org}



containing both chromium oxide and calcium phosphate, while that formed in NaCl contains only oxide.

3.3 Chemical composition and thickness of the layers formed in NaCl and simulated Hanks' physiological solution containing hyaluronic acid

The effect of hyaluronic acid (HA), added at two different concentrations 1 and 4 g/L, on the formation of surface layers after immersion of CoCrMo alloy was studied in NaCl and in HS during 15 h immersion at the E_{oc} . The addition of HA affects the composition of the surface layers formed in both NaCl and HS but the effect in the presence of the latter is considerably larger (Table 2). The addition of HA results in a twofold decrease in concentration of metal components, and the appearance of nitrogen. In HS, the addition of HA leads to the complete disappearance of Co and Mo components and the minimization of Cr. At the same time the concentrations of Ca and P increase, resulting in a Ca/P ratio of 1.16 (compared to 0.76 in plain HS). The increase in HA concentration from 1 to 4 g/L does not affect the Ca/P ratio. The concentrations of carbon and oxygen did not change significantly in the presence of HA but, as will be seen below, the chemical speciation of

these elements changed. Therefore, it appears that the presence of HA in NaCl causes a thinning, a slower formation of oxide film, or the HA becomes covered by the layer containing nitrogen which prevents its full detection. In HS, a layer of calcium phosphate is formed which is clearly thick enough to prevent the detection of oxide underneath.

Normalized XPS high resolution spectra recorded at the surfaces of samples immersed in NaCl and HS, with and without the presence of two concentrations of HA, are presented in Figs. 3, 4, and 5. The addition of HA to NaCl leads to a decrease in the metal concentration (Table 2) but induces no significant change in the shape spectra Cr 2p, Co 2p and Mo 3d (Fig. 3). Interesting features are observed in non-metal components. The addition of HA to NaCl induces the appearance of a new peak in the O 1s spectra at 533.1 eV, a new peak in the C 1s spectra at 287.0 eV, and a nitrogen peak at 400.5 eV (Fig. 4). These results confirm that the surface layer formed on CoCrMo alloy in NaCl containing HA comprises mainly chromium oxide, but that it differs from that formed in the absence of HA since it contains additional carbon-, oxygen- and nitrogen-species, clearly originating from organic material [35], in this case from HA.

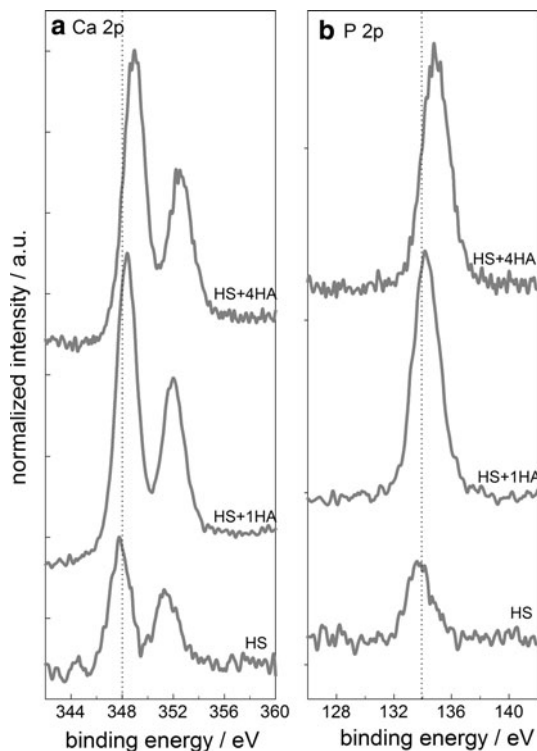


Fig. 5 Normalized XPS **a** Ca 2p and **b** P 2p spectra recorded at the layer formed on CoCrMo alloy after 15 h immersion in 0.9 % NaCl and Hanks’ simulated physiological solution (HS) with and without addition of 1 and 4 g/L hyaluronic acid (HA). Dashed lines denote the centres of peaks

In the presence of HA in HS no metal components could be detected (Fig. 3). The surface contains mainly calcium phosphate (Fig. 5). The centres of Ca 2p and P 2p peaks are shifted to higher binding energy as the HA concentration is increased. For Ca 2p, the peak centre shifts from 347.7 eV in plain HS to 348.4 and 349.0 eV in the presence of 1 and 4 g/L HA, i.e. by 1.3 eV. For P 2p, the peak centre shifts from 133.6 eV in plain HS to 134.1 and 134.7 eV in the presence of 1 and 4 g/L HA, i.e. by 1.1 eV. Feng et al. [36] observed the shift of the Ca 2p and P 2p peaks in apatite coatings formed in the presence of bovine serum albumin and ascribed it to chemical bonding between Ca²⁺ and PO₄³⁻ and protein. It is mostly accepted that proteins interact with apatite through Ca²⁺ [21, 37, 38], but PO₄³⁻ may also provide a driving force for protein adsorption [39]. It was suggested that albumin could adsorb to the apatite through lateral interaction in a covalent bond, since PO₄³⁻ ions are negatively charged and electrostatic effects would not be the dominant factor as in the case of Ca²⁺ ions [36]. The significant chemical shift observed in the present work for Ca and P peaks indicate that a similar mechanism may be operative, i.e. chemical bonding of hyaluronic acid components with calcium phosphate. This will be further discussed below.

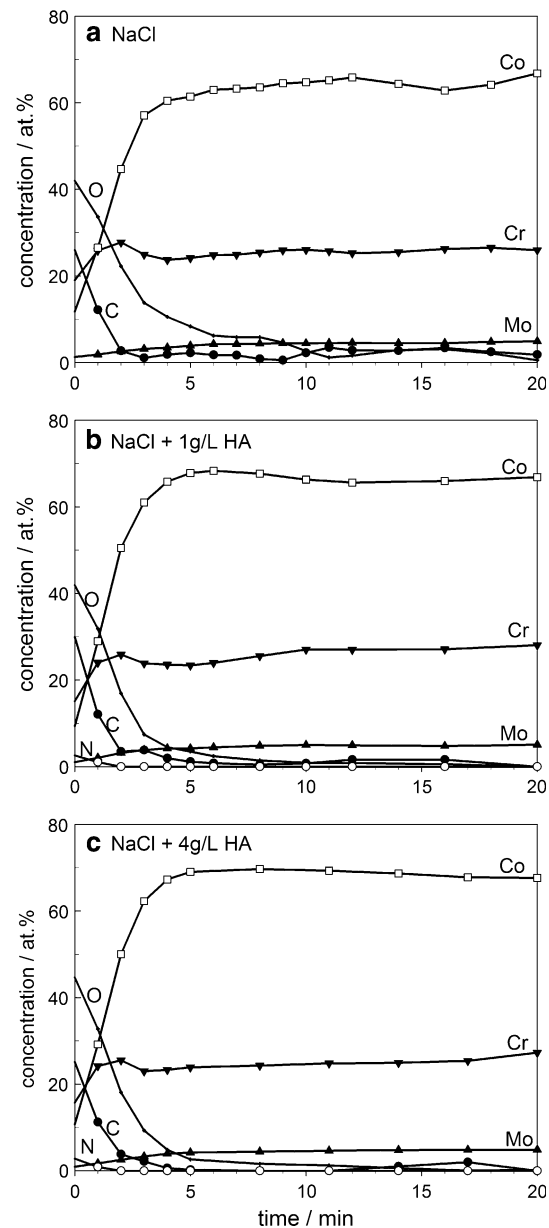


Fig. 6 Sputter depth profiles of layers formed on CoCrMo alloy after 15 h immersion in 0.9 % NaCl with and without addition of 1 and 4 g/L hyaluronic acid (HA). Sputter rate 2.0 nm/min relative to the SiO₂ standard

In HS containing HA the centre of the O 1s peak also shifts to higher binding energy, 532.9 eV, and, in contrast to NaCl, no new peak at 533.1 eV is observed (Fig. 4a). The binding energy of oxygen in calcium phosphate was found to be higher (531.6–531.8 eV) than that of oxygen in chromium oxide (529.8–530.8 eV) [32], which agrees well with the present results. The changes in carbon spectra are also less pronounced than those in NaCl, where a new peak appears at 287.0 eV (Fig. 4b). In HS, the centre of the C1s peak is shifted to even higher binding energy, 288.0 eV.

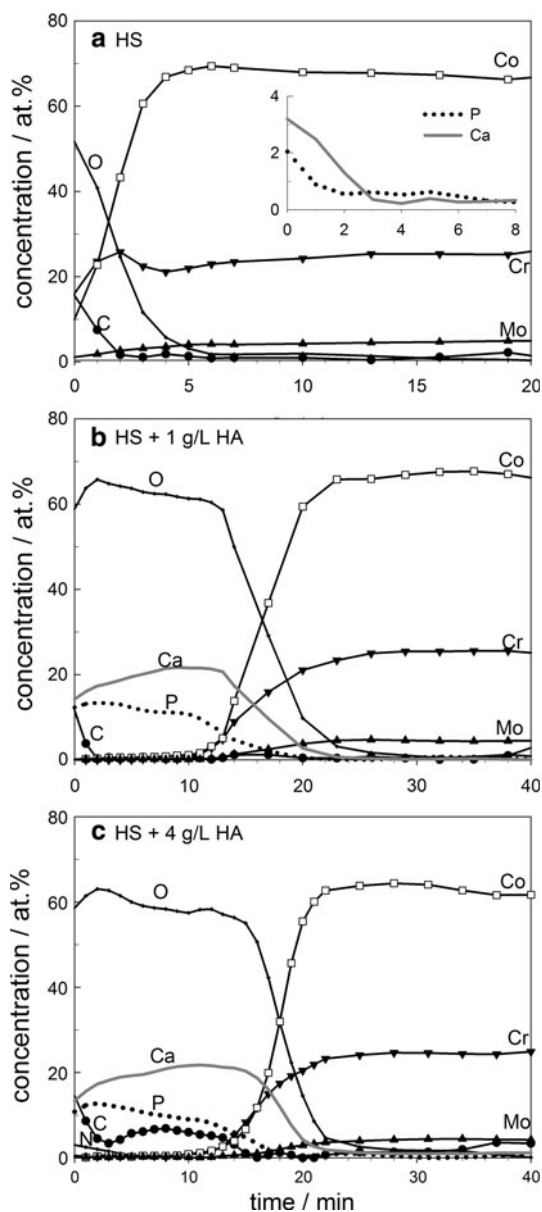


Fig. 7 Sputter depth profiles of layers formed on CoCrMo alloy after 15 h immersion in simulated Hanks' physiological solution (HS) with and without addition of 1 and 4 g/L hyaluronic acid (HA). Inset in **a** depicts the y-axis with expanded scale. Sputter rate 2.0 nm/min relative to the SiO₂ standard

Depth profiles of the surface layers formed in the presence of HA are presented in Figs. 6 and 7. In NaCl, the profiles remain virtually unchanged. The oxide thickness decreases from 4.6 nm in NaCl to 3.6 and 3.2 nm in the presence of 1 and 4 g/L HA (Fig. 6b, c). In HS, however, the addition of HA induced an almost tenfold increase in layer thickness: it increased from 3.6 nm in HS to 32.8 and 36.4 nm in the presence of 1 and 4 g/L HA (Fig. 7b, c). Calcium and phosphorus, which were minor elements in plain HS (Fig. 7a), are now major components of the layer. Another issue is noteworthy, namely that, in the presence

of higher HA concentration, the carbon profile follows a trend similar to those of Ca and P, indicating that carbon is incorporated in this layer throughout its depth (Fig. 7c). This was not observed after addition of the lower HA concentration (Fig. 7b) or in NaCl, where the intensity of carbon decreased as soon as the sputter process began (Fig. 6b, c). In addition to the data presented in Fig. 5, this is the evidence that, in the presence of HA, the chemical environment of carbon in the layer formed in HS differs from that when the layer is formed in NaCl. It appears that in HS both carbon and oxygen are chemically bonded to calcium phosphate, whilst in NaCl carbon is present mainly on the top of the layer.

As the layer was progressively sputtered away, the intensities of Ca, P, O, N and C signals decreased and metal components appeared at the layer/alloy interface. The XPS spectra were recorded at each depth of the layer (results not shown). As the Cr 2*p* peak appeared, the peak centre was located in the oxide range, and then immediately shifted to the metal range. This means that, after sample preparation, the surface was spontaneously covered by a thin layer of chromium oxide after exposure to air. Once immersed in HS containing HA, this oxide layer did not grow further but, instead, a thick layer of calcium phosphate was formed above it. In contrast to Cr, cobalt and molybdenum appear, mainly as metals, at the interface, in accordance with chromium oxide being the predominant component of the spontaneously formed layer on CoCrMo alloy.

3.4 Structure of the sub-surface layer formed in NaCl and simulated Hanks' physiological solution, both containing hyaluronic acid

Angle resolved XPS (AR-XPS) measurements were carried out for surface layers formed following 15 h immersion of CoCrMo alloy in NaCl and HS containing 1 and 4 g/L HA. The aim was to determine whether oxide, phosphate and organic containing species are distributed differently at the sub-surface region.

In NaCl and HS, and in NaCl containing HA, the intensity of the metal part of Cr 2*p* at 574.2 eV was more intense at higher take-off angle (i.e. closer to the inner interface), while it was not visible closer to the surface (results not shown). This dependence confirms that the chromium oxide layer is only a few nanometres thick, thus being sensitive to change in the take-off angle [23]. This is a common result observed for a surface covered by an oxide layer. In HS containing HA no metal signal could be detected (Fig. 4). Instead, calcium and phosphorus spectra were identified and these spectra did not change as a function of take-off angle, indicating that the composition of phosphate is homogeneous throughout the layer depth

investigated by AR-XPS. Interesting results are obtained for non-metal elements—carbon and oxygen—in their relation to the formation of organic-containing compounds (Figs. 8, 9). In plain NaCl and HS the C 1s peak is related to the presence of aliphatic carbon at 284.8 eV (Fig. 8a, b). The peak intensity and shape are not sensitive to the take-off angle. The addition of HA changes the shape of the spectrum (Fig. 8c, d). Only spectra at higher HA concentration are considered—those recorded at lower HA concentration lie between these two extreme cases (0 and 4 g/L). On addition of 4 g/L HA to NaCl the peak centre is shifted to higher binding energy by almost 2 eV (to 287.4 eV), clearly due to the formation of species originating from HA (Fig. 8c). Spectra are not changed significantly with increasing take-off angle. In HS, however, the intensity of the C 1s peak at the higher binding energy of 288.1 eV (related to the C–N and C–O organic species) increases with increasing take-off angle (i.e., closer to the bulk), indicating that carbon is incorporated throughout the depth of the calcium phosphate layer (Fig. 8d).

In plain NaCl and HS, the O 1s peak is related to the presence of oxide/hydroxide oxygen (Fig. 9a, b) and, like carbon, is not sensitive to changes in take-off angle. The addition of HA to HS induces a shift of the peak centre to higher binding energy of 532.9 eV, in agreement with the formation of phosphate; the shape of the peak remains narrow (Fig. 9d). In NaCl, however, two peaks at 532.6 and 533.4 eV are clearly visible in the presence of HA (Fig. 9c), presumably related to the formation of oxide and organic-containing species. The latter are enriched at the surface, since the peak at higher E_b prevails at 20°. The N 1s peak (Fig. 4c) is not sensitive to changes in take-off angle (results not shown).

3.5 Chemical composition and thickness of the layers formed in simulated Hanks' physiological solution containing hyaluronic acid—the effect of immersion time

The effect of immersion time at E_{oc} (1 and 15 h) on the composition and thickness of the layers formed on CoCrMo alloy was investigated in HS, with and without the addition of 4 g/L HA (Fig. 10). The composition deduced from XPS survey spectra recorded at the surface of the layers is presented in Table 3. Increase in t_{imm} does not affect significantly the depth profiles in plain HS (Fig. 10a, b). The thickness of the oxide layer is 1.5 and 2.1 nm after 1 and 15 h immersion. In both cases the surface contains more phosphorus than calcium (inserts in Fig. 10a, b), giving ratios of Ca/P of 0.39 and 0.74, respectively (Table 3). The prevailing concentration of P at the beginning of immersion may be evidence that PO_4^{3-} ions adsorb first at the surface of chromium oxide, similarly

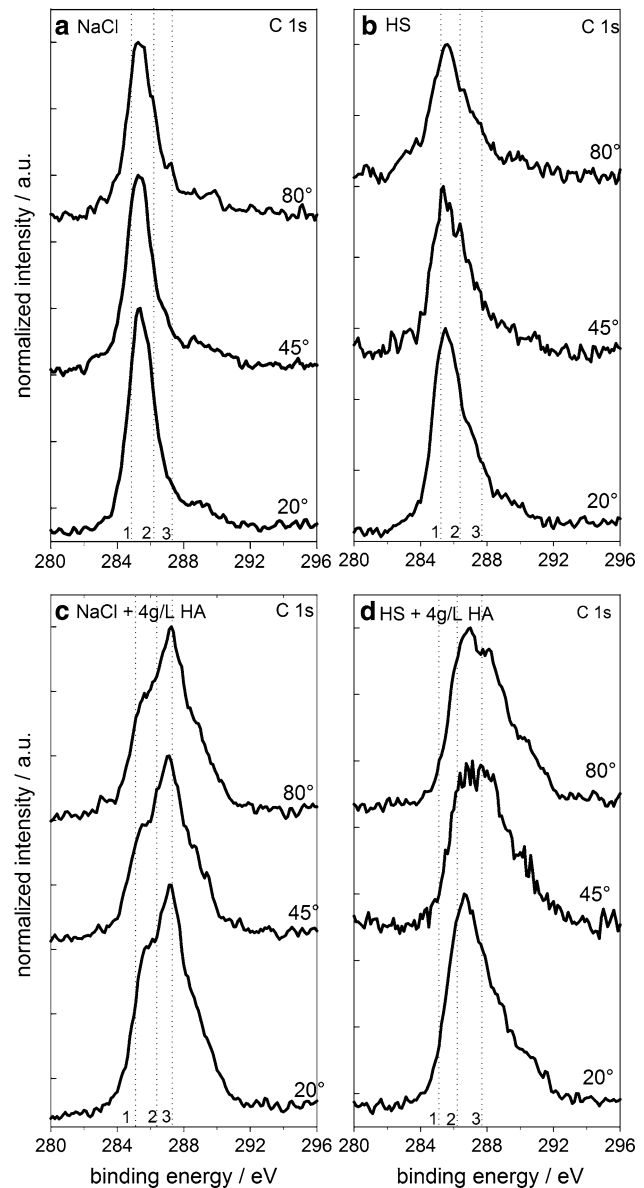


Fig. 8 Normalized XPS C 1s spectra recorded at the layer formed on CoCrMo alloy after 15 h immersion in 0.9 % NaCl and Hanks' simulated physiological solution (HS), with and without addition of 4 g/L hyaluronic acid (HA). Spectra were recorded at different take-off angles (20°, 45° and 80°). Dashed lines denote the positions of (1) C–C, C–H (2) C–O and (3) C_{org}

to their adsorption at the surface of titanium oxide [33, 34]. This initially adsorbed phosphate layer attracts negatively charged Ca^{2+} ions, leading, with time, to the formation of calcium phosphate with increased Ca/P ratio.

After 1 h immersion in the presence of HA the thickness of the layer increased to 3.2 nm (compared to 1.5 nm in plain HS) (Fig. 10c). Now Ca prevails over P, in contrast to plain HS. The Ca/P ratio is 0.95, already higher than in plain HS after 15 h immersion (Table 3). Besides oxide and phosphate the layer also contains nitrogen (inset in Fig. 10c). An increase in immersion time to 15 h

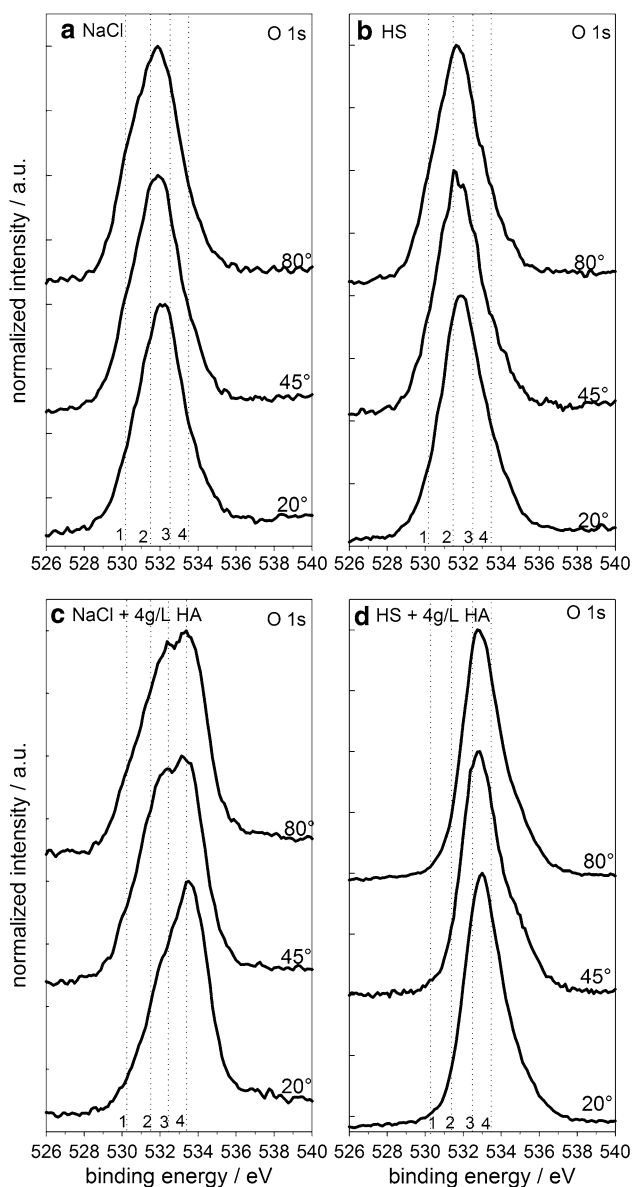


Fig. 9 Normalized XPS O 1s spectra recorded at the layer formed on CoCrMo alloy after 15 h immersion in 0.9 % NaCl and Hanks' simulated physiological solution (HS) with and without addition of 4 g/L hyaluronic acid (HA). Spectra were recorded at different take-off angles (20°, 45° and 80°). Dashed lines denote the positions of (1) O^{2-} (2) OH^- (3) PO_4^{3-} (4) O_{org}

significantly changes the composition and thickness of the layer which now amounts to 19.4 nm (Fig. 10d). The layer contains primarily calcium phosphate mixed with nitrogen and carbon, whose concentration increases sharply compared to that after 1 h immersion. The Ca/P ratio amounts to 1.22. These data prove that the presence of hyaluronic acid strongly stimulates the formation of calcium phosphate on CoCrMo alloy. The most important role in this process is probably played by Ca^{2+} ions. Calcium ions increase the flexibility of the chain by promoting a greater

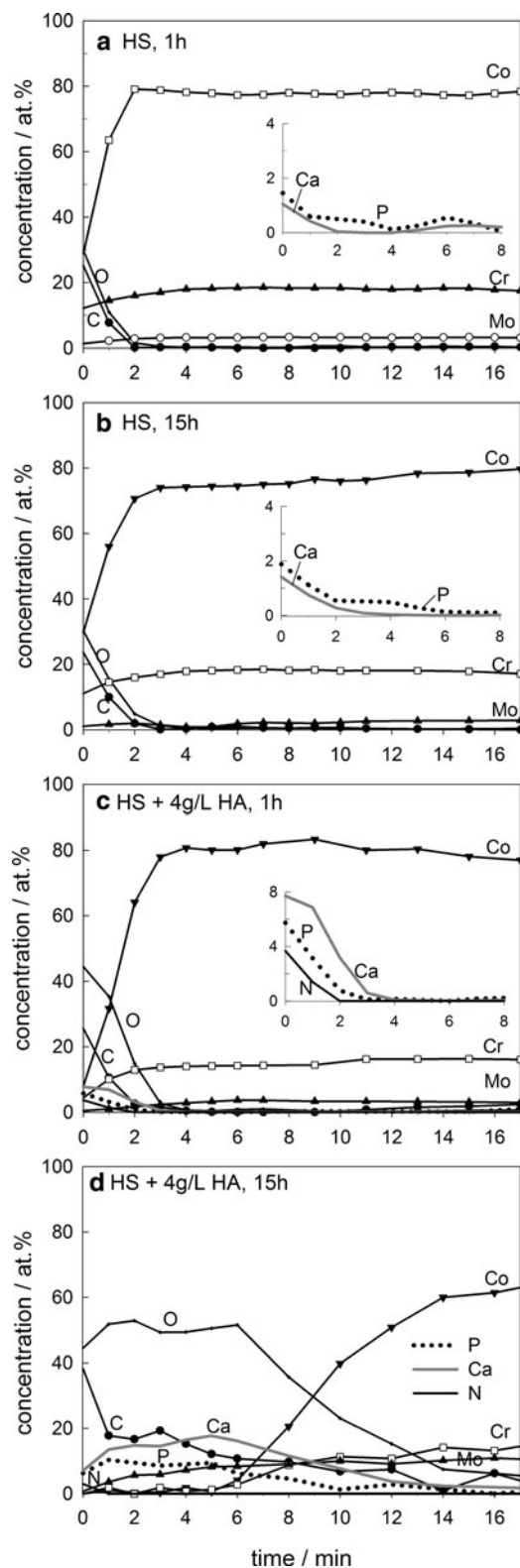


Fig. 10 Sputter depth profiles of layers formed on CoCrMo alloy after immersion in (a, b) Hanks' simulated physiological solution (HS) for a 1 h and b 15 h, and c, d HS containing 4 g/L hyaluronic acid (HA) for c 1 h and d 15 h. Insets in (a–c) depict the y-axis with expanded scale. Sputter rate 2.0 nm/min relative to the SiO_2 standard

Table 3 Composition of layers formed on CoCrMo alloy after 1 and 15 h immersion in simulated Hanks' physiological solution (HS) with and without addition of 4 g/L hyaluronic acid (HA).

Element	Concentration/at%			
	HS		HS+HA	
	1 h	15 h	1 h	15 h
O 1s	49.7	44.2	41.7	40.4
C 1s	27.0	35.0	35.9	39.1
Cr 2p	12.6	8.3	1.5	1.3
Co 2p	5.2	–	1.7	<0.1
Mo 3d	1.2	1.2	0.2	0.6
N 1s	–	–	5.3	3.9
Mg 2s	–	–	–	2.5
Si 2p	–	5.9	–	–
P 2p	3.1	3.1	6.3	5.5
Ca 2p	1.2	2.3	6.0	6.7
Ca/P	0.39	0.74	0.95	1.22

Composition was deduced from XPS survey spectra

range of movement at each glycosidic bond [18]. It was proposed that, in the presence of Ca^{2+} , there is less stability in the range of hydrogen bonds that bridge adjacent sugars in these linkages. Individual Ca^{2+} or Mn^{2+} ions may co-ordinate two carboxyl groups on the same HA chain and promote chain contraction [40]. Molecular dynamics simulations predict that various conformations of HA may be present in solution, e.g. a fourfold structure, a hollow helix or “hairpin” structure [41]. Although not proven experimentally, these ordered conformations could rapidly exchange in the HA chain, thus contributing to its flexibility and solubility.

Ca^{2+} ions change the conformation of HA, which becomes a three-fold helix and less rigid [19]. It can be hypothesized that HA chains may be disrupted to smaller units of disaccharides. Degradation of HA by an electrochemical process leads to the formation of carbonyl and carboxyl groups [42]. The formation of a new peak in the C 1s signal at 287.0–288.0 eV in the presence of HA may be ascribed to the formation of these groups following the degradation of hyaluronic acid. Evidently, due to the presence of Ca^{2+} ions, the HA chain becomes more reactive, eventually resulting in the formation of calcium phosphate, which is strongly stimulated in the presence of HA. It appears that HA bonds chemically to calcium phosphate throughout its depth. In solutions that contain no Ca^{2+} ions (i.e. NaCl) only a thin layer containing elements originating from HA is formed on top of the chromium oxide layer.

Degradation of hyaluronic acid is relevant from the biological point of view. It is well established that the large

molecular weight of HA is important in many biological processes [16, 18, 42]. However, low molecular mass HA and fragments of HA are also important. Recently, low molecular weight HA has been implicated in several biological processes, including angiogenesis, cell proliferation, maturation, migration, activation of protein tyrosine kinase cascades, and inflammatory gene expression [43–45]. In vivo, at sites of inflammation, high molecular weight HA (M_r 2–6 $\times 10^6$ Da) can be depolymerized to lower molecular weight (M_r 0.2 $\times 10^6$ Da) fragments by oxygen radicals and enzymatic degradation by hyaluronidase, β -glucuronidase, and hexosaminidase [44]. These lower molecular weight fragments may activate an innate immune response and act as an endogenous danger signal alerting the immune system of a breach in tissue integrity [44]. Partial degradation products of sodium hyaluronate induce an angiogenic response (formation of new blood vessels), thus contributing to wound healing [45]. The activity is restricted to hyaluronate fragments between 4 and 25 disaccharides in length.

3.6 Morphology of the layers formed in NaCl and simulated Hanks' physiological solution containing hyaluronic acid

FE-SEM images of layers formed on the CoCrMo alloy following 15 h immersion in plain NaCl and HS and in NaCl and HS with the addition of 1 and 4 g/L HA are presented in Figs. 11 and 12. The surface and depth compositions of the related layers are given in Figs. 4, 5, 6 and 7. After immersion in plain NaCl the surface still shows the grinding marks (Fig. 11a), which is understandable since the thickness of the oxide layer is only 4.6 nm (Fig. 6a). Similar characteristics are observed at the surface of CoCrMo immersed in HS (Fig. 12a). The addition of 1 and 4 g/L HA to NaCl does not change the surface morphology significantly (Fig. 11b–d). On the other hand, the addition of only 1 g/L HA induces the formation of a dense, homogeneous layer (Fig. 12b), which corresponds to the calcium phosphate (see depth profile in Fig. 7b). The increase in HA concentration leads to the formation of a layer that is homogeneous, even at the nano-sized level (Fig. 12c, d).

3.7 Cell viability and alkaline phosphatase activity of simulated physiological solution containing hyaluronic acid exposed to CoCrMo alloy

These experiments were performed in Hanks' simulated physiological solution (HS) with (HS+HA) and without (HS) the addition of hyaluronic acid. To determine the effect of exposure to CoCrMo alloy, the CoCrMo samples were immersed in these two solutions for 24 h (denoted as

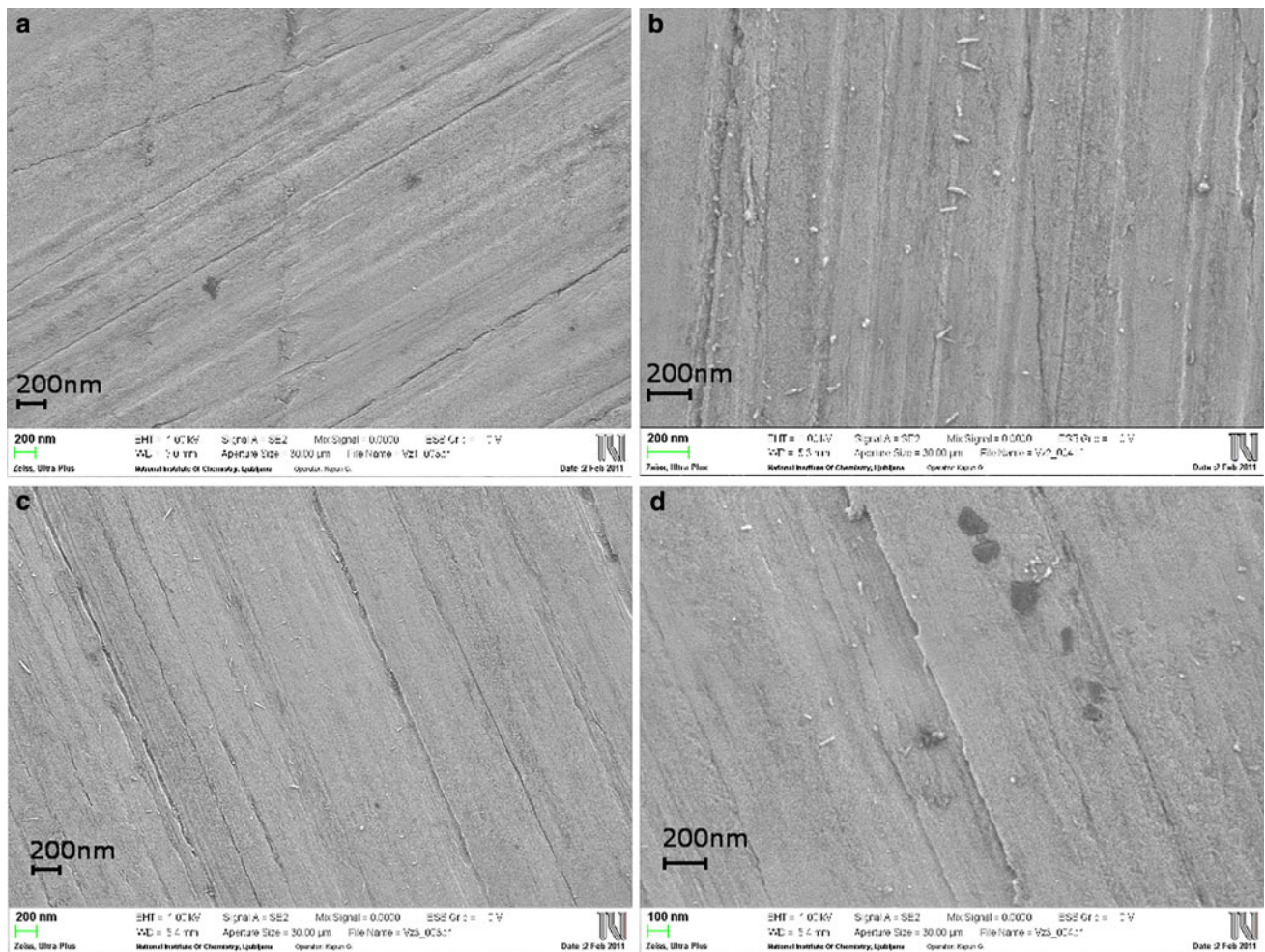


Fig. 11 FE-SEM images recorded at the surface of CoCrMo alloy after 15 h immersion in **a** 0.9 % NaCl **b** NaCl containing 1 g/L hyaluronic acid (HA), and **c**, **d** NaCl containing 4 g/L hyaluronic acid (HA). Magnification (**a**, **c**) $\times 50,000$ (**b**, **d**) $\times 100,000$

HS+alloy and HS+HA+alloy). For cell viability assessment, HOS cells were grown in a mixture of 1/3 test samples and 2/3 complete growth medium for 3 days, followed by the Alamar Blue[®] assay. Cell viability was measured using the Alamar Blue[®] assay. When comparing the average fluorescence generated by the cells exposed to test solutions (HS, HS+HA, HS+alloy, HS+HA+alloy) and to the control solution (2/3 growth medium and 1/3 PBS), no statistically significant differences were observed (P values ranged between 0.315 and 0.846) (Fig. 13). Thus, none of the test solutions affected HOS cell survival.

ALP activity was evaluated by measuring fluorescence of the fluorogenic substrate MUP. Although ALP activities varied after exposure to the test solutions (Fig. 14), no statistically significant differences were observed between cells exposed to HA and control (unexposed) cells (P values ranged from 0.290–0.963). However, after 24 h immersion of the CoCrMo sample, the ALP activity in

cells exposed to the solution containing hyaluronic acid (HS+HA+alloy) was significantly greater ($P = 0.040$) than in its absence (HS+alloy). Since ALP is a well-established marker for the initial stages of osteoblast differentiation, this result indicates that the cells' response to hyaluronic acid is beneficial in terms of the mechanism of bone cell function and matrix production/turnover. This result further supports the observed enhanced formation of the calcium phosphate layer in simulated physiological solution containing hyaluronic acid (Figs. 7, 10). Recently, several reports have been published indicating the positive effect of hyaluronic acid in different conditions [46–50]. Hyaluronic acid-based hydrogels functionalized with heparin exhibit an increased ALP activity indicating increased osteogenic activity [46]. Similar results were obtained for a collagen/hyaluronic acid polyelectrolyte membrane coating crosslinked with functionalized Arg-Gly-Asp (RGD) peptide on titanium [47], titanium surface functionalized with

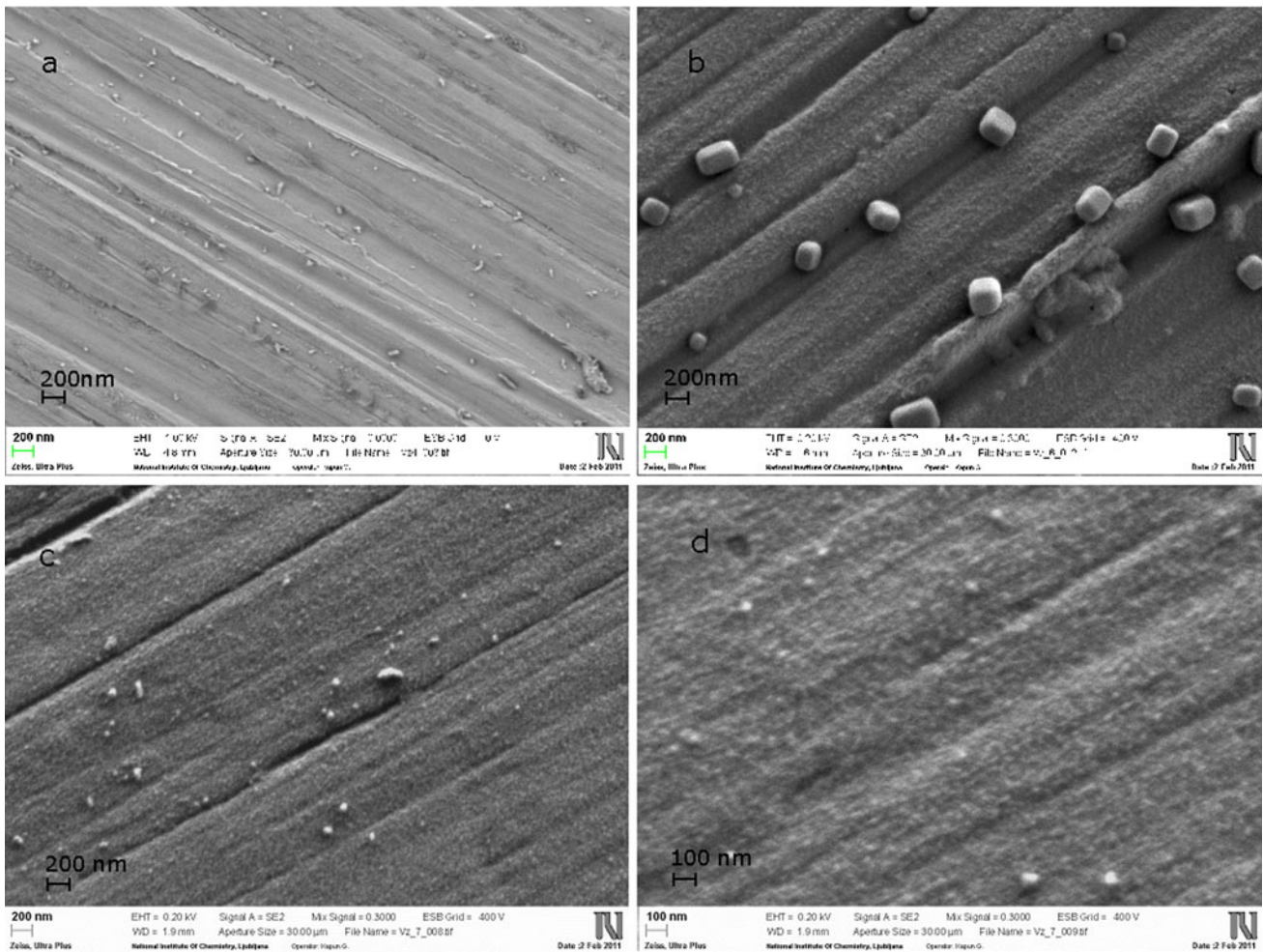


Fig. 12 FE-SEM images recorded at the surface of CoCrMo alloy after 15 h immersion in **a** simulated Hanks’ physiological solution (HS) **b** HS containing 1 g/L hyaluronic acid (HA), and **(c,d)** HS containing 4 g/L hyaluronic acid (HA). Magnification **(a, b, c)** $\times 50,000$ **d** $\times 100,000$

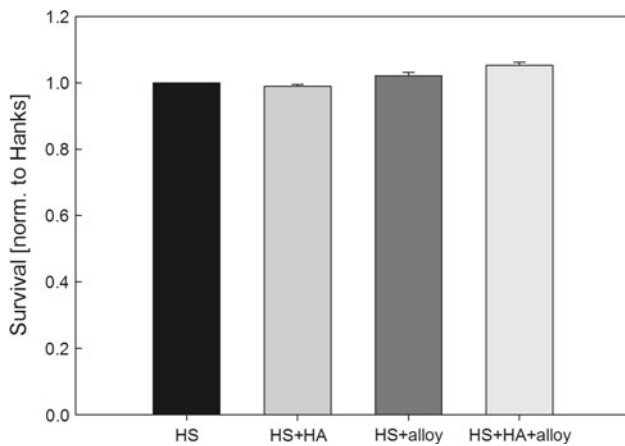


Fig. 13 Survival of HOS cells normalized to survival of Hanks’ solution-exposed controls: Hanks’ solution (HS), solution containing 4 g/L hyaluronic acid (HS+HA), solution after 24 h immersion of the CoCrMo alloy (HS+alloy), and solution containing 4 g/L hyaluronic acid after 24 h immersion of the CoCrMo alloy (HS+HA+alloy)

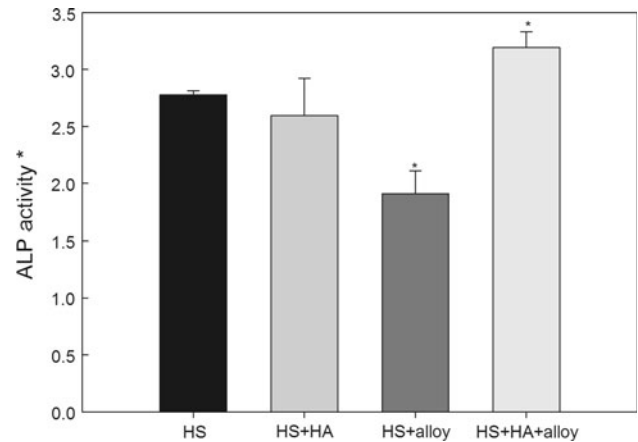


Fig. 14 ALP activity in HOS cells after exposure to the test solutions: solution (HS), solution containing 4 g/L hyaluronic acid (HS+HA), solution after 24 h immersion of the CoCrMo alloy (HS+alloy), and solution containing 4 g/L hyaluronic acid after 24 h immersion of the CoCrMo alloy (HS+HA+alloy)

HA/chitosan polyelectrolyte multilayers coupled with RGD peptide [48], poly(lactic-co-glycolic acid) grafted HA [49] and poly(L-lactic acid) modified with heparin and HA [50].

4 Conclusions

The behaviour of CoCrMo alloy in two simulated physiological solutions, NaCl and Hanks' solution, containing hyaluronic acid has been investigated. Hyaluronic acid is an important component of synovial fluid, the natural environment of metal prostheses. Its effect is significant, especially in simulated Hanks' physiological solution containing inorganic salts. It results in the formation of a thick layer of calcium phosphate, which is approximately ten times thicker than that in the absence of hyaluronic acid. Due to its formation, the underlying layer of chromium oxide cannot be detected. The presence of Ca^{2+} and PO_4^{3-} ions is essential for the interaction between the chromium oxide surface and the hyaluronic chain. It is hypothesized that Ca^{2+} promotes the cleavage of hyaluronic acid to smaller units which then react chemically with calcium phosphate, as indicated by the chemical shift in the related XPS peaks. After longer immersion periods, carbon and nitrogen are found to be incorporated throughout the depth of the calcium phosphate layer. This layer is homogeneous at the nano-level. Angle-resolved measurements prove the formation, related to hyaluronic acid, of new species in oxygen, carbon and nitrogen spectra. In NaCl solution, species originating from hyaluronic acid are mixed with the chromium oxide layer.

The effect of immersion time on the thickness of the layer is greater when formed in the presence of hyaluronic acid than plain solution. Electrochemically this effect is reflected in the shift of the corrosion potential and the decrease in the current density in the potentiodynamic polarization curves.

Under the experimental conditions used the addition of hyaluronic acid does not statistically significantly affect the viability of osteoblast-like cells but does increase the activity of alkaline phosphatase, indicating its beneficial effect on osteogenic activity.

The present results thus suggest the potential for increasing the osseointegration capability of CoCrMo alloy.

Acknowledgments The authors thank Mojca Seručnik, BSc, and Gregor Žerjav, BSc, for valuable experimental work, Gregor Kapun, BSc, of the National Institute of Chemistry for expertise in the FE-SEM analysis, Dr. Janez Kovač for valuable comments on XPS measurements, and dr. Antonija Lesar for fruitful discussions. Human osteosarcoma (HOS), a human osteoblast-like cell line, was kindly donated by prof. Janja Marc, Faculty of Pharmacy, University of Ljubljana. Financial support by the Slovenian Research Agency is acknowledged (Grants No. J1-2243 and J1-4136).

References

1. Kasemo B. Biological surface science. *Surface Sci.* 2002;500:656–77.
2. Puleo DA, Nanci A. Understanding and controlling the bone-implant interface. *Biomaterials.* 1999;20:2311–21.
3. Xu T, Zhan N, Nichols HL, Shi D, Wen X. Modification of nanostructured materials for biomedical applications. *Mater Sci Eng C.* 2007;27:579–94.
4. Paital SR, Dahotre NB. Calcium phosphate coatings for bio-implant applications: materials, performance factors and methodologies. *Mater Sci Eng R.* 2009;66:1–70.
5. Igual Muñoz A, Mischler S. Interactive effects of albumin and phosphate ions on the corrosion of CoCrMo implant alloy. *J Electrochem Soc* 2007;154: C562-70.
6. Hodgson AWE, Kurz S, Virtanen S, Fervel V, Olsson C-OA, Mischler S. Passive and transpassive behaviour of CoCrMo in simulated biological solutions. *Electrochim Acta.* 2004;49:2167–78.
7. Li Y-S, Wang K, He P, Huang BX, Kovacs P. Surface-enhanced Raman spectroelectrochemical studies of corrosion films on implant Co–Cr–Mo alloy in biosimulating solutions. *J Raman Spectrosc.* 1999;30:97–103.
8. Milošev I, Strehblow HH. The composition of the surface passive film formed on CoCrMo alloy in simulated physiological solution. *Electrochim Acta.* 2003;48:2767–74.
9. Milošev I. Surface treatments for biomedical applications. In: Djokic Stojan S, editor. *Modern aspects of electrochemistry*, vol 55. Springer; 2012. p. 1–72.
10. Hanawa T, Hiromoto S, Asami K. Characterization of the surface oxide film of a Co–Cr–Mo alloy after being located in quasi-biological environments using XPS. *Appl Surf Sci.* 2001;183:68–75.
11. Contu F, Elsener B, Böhni H. Characterization of implant materials in fetal bovine serum and sodium sulfate by electrochemical impedance spectroscopy. I Mechanically polished samples. *J Biomed Mater Res.* 2002;62:412–21.
12. Hiromoto S, Noda K, Hanawa T. Development of electrolytic cell with cell-culture for metallic biomaterials. *Corrosion Sci.* 2002;44:955–65.
13. Cheng X, et al. Corrosion behaviour of titanium in the presence of calcium phosphate and serum proteins. *Biomaterials.* 2005;26:7350–6.
14. Milošev I. The effect of biomolecules on the behaviour of CoCrMo alloy in various simulated physiological solutions. *Electrochim Acta.* 2012;78:259–73.
15. Yadav KL, Brown PW. Formation of hydroxyapatite in water, Hank's solution, and serum at physiological temperature. *J Biomed Mater Res A.* 2003;65A:158–63.
16. Day AJ, Sheenan JK. Hyaluronan: polysaccharide chaos to protein organisation. *Curr Opin Chem Biol.* 2001;11:617–22.
17. Barbucci R, Lamponi S, Borzacchiello A, Ambrosio L, Fini M, Torricelli P, Giardino R. Hyaluronic acid hydrogel in the treatment of osteoarthritis. *Biomaterials.* 2002;23:4503–13.
18. Gribbon P, Heng BC, Hardingham TE. The analysis of intermolecular interactions in concentrated hyaluronan solutions suggest no evidence for chain–chain association. *Biochem J.* 2000;350:329–35.
19. Sheehan JK, Atkins EDT. X-ray fibre diffraction study of conformational changes in hyaluronate induced in the presence of sodium, potassium and calcium cations. *Int J Biol Macromol.* 1983;5:215–21.
20. Collis JJ, Embery G. Adsorption of glycosaminoglycans to commercially pure titanium. *Biomaterials.* 1992;13:548–52.
21. Ellingsen JE. A study on the mechanism of protein adsorption to TiO_2 . *Biomaterials.* 1991;12:593–6.

22. Hanawa T, Ota M. Calcium phosphate naturally formed on titanium in electrolyte solution. *Biomaterials* 1991;12:767–14.
23. Briggs D, Rivière JC. Spectral interpretation. In: Briggs D, Seah MP, editors. *Practical surface analysis by XPS and AES*. New York: Chichester; 1990.
24. Seah MP. Summary of ISO/TC 201 standard: ISO 14701:—surface chemical analysis—X-ray photoelectron spectroscopy—measurement of silicon oxide thickness. *Surf Interface Anal*. 2012;44:876–8.
25. Pan J, Thierry D, Leygraf C. Electrochemical impedance spectroscopy study of the passive film on titanium for implant applications. *Electrochim Acta*. 1996;41:1143–53.
26. Aziz-Kerrzo, Conroy KG, Fenelon AM, Farrell ST, Breslin CB. Electrochemical studies on the stability and corrosion resistance of titanium-based implant materials. *Biomaterials* 2001;21:1531–9.
27. Souto RA, Laz MM, Reis RL. Degradation characteristics of hydroxyapatite coatings on orthopedic TiAlV in simulated physiological media investigated by electrochemical impedance spectroscopy. *Biomaterials*. 2003;24:4213–21.
28. Hodgson AWE, Mueller Y, Forster D, Virtanen S. Electrochemical characterisation of passive films on Ti alloys under simulated biological conditions. *Electrochim Acta*. 2002;47:1913–23.
29. Tamilselvi S, Raman V, Rajendran N. Corrosion behaviour of Ti-6Al-7Nb and Ti-6Al-4 V ELI alloys in the simulated body fluid solution by electrochemical impedance spectroscopy. *Electrochim Acta*. 2006;52:839–46.
30. Metikoš-Huković M, Pilić Z, Babić R, Omanović D. Influence of alloying elements on the corrosion stability of CoCrMo implant alloy in Hank's solution. *Acta Biomater*. 2006;2:693–700.
31. Milošev I, Blejan D, Varvara S, Muresan LM. Effect of anodic oxidation on the corrosion behaviour of Ti-based materials in simulated physiological solution. submitted.
32. Wagner CD, Naumkin AV, Kraut-Vass A, Allison JW, Powell CJ, Rumble JR Jr. NIST X-ray photoelectron spectroscopy database, NIST standard reference database 20, Version 3.5, Data compiled and evaluated. <http://srdata.nist.gov/xps/>.
33. Tsutsumi Y, Nishimura D, Doi H, Nomura H, Hanawa T. Difference in surface reactions between titanium and zirconium in Hank's solution to elucidate mechanism of calcium phosphate formation on titanium using XPS and cathodic polarization. *Mat Sci Eng C* 2009; 29:1702–8.
34. Frauchiger L, Taborelli M, Aronsson B-O, Descouts P. Ion adsorption on titanium surfaces exposed to a physiological solution. *Appl Surf Sci*. 1999;143:67–77.
35. Milošev I, Jovanović Ž, Bajat JB, Jančić-Heinemann J, Mišković-Stanković VB. Surface analysis and electrochemical behaviour of aluminium pretreated by vinyltriethoxysilane films in mild NaCl solution. *J Electrochem Soc*. 2012;159:C303–11.
36. Feng B, Chen J, Zhang X. Interaction of calcium and phosphate in apatite coating on titanium with serum albumin. *Biomaterials*. 2002;23:2499–507.
37. Hughes Wassell DT, Graham E. Adsorption of bovine serum albumin on to titanium powder. *Biomaterials* 1996;17:859–64.
38. Steinberg D, Klinger A, Kohavi D, Sela MN. Adsorption of human salivary proteins to titanium powder I: adsorption of human salivary albumin. *Biomaterials*. 1995;16:1339–43.
39. Hay DI, Moreno EC. Differential adsorption and chemical affinities of protein for apatitic surfaces. *J Dent Res*. 1979;58:930–40.
40. Sheenan JK, Brass A, Almond A. The conformations of hyaluronan in aqueous solution: comparison of theory and experiment. *Biochem Soc Trans*. 1999;27:121–4.
41. Almond A, Brass A, Sheenan JK. Deducing polymeric structure from aqueous molecular dynamics simulations of oligosaccharides: predictions from simulations of hyaluronan tetrasaccharides compared with hydrodynamic and X-ray fibre diffraction data. *J Mol Biol*. 1998;284:1425–37.
42. Gu Z, Cai Q, He Y, Fu T, Li F. Degradation of hyaluronan by an electrochemical process. *Carbohydr Polym*. 2010;82:521–3.
43. Taylor KR, Trowbridge JM, Rudisill JA, Termeer CC, Simon JC, Galo RL. Hyaluronan fragments stimulate endothelial recognition of injury through TLR4. *J Biol Chem*. 2004;279:17079–84.
44. Scheibner S, Lutz MA, Boodoo S, Fenton MJ, Powell JD, Horton MR. Hyaluronan fragments act as an endogenous danger signal by engaging TLR2. *J Immun*. 2006;177:1272–81.
45. West DC, Hampson IN, Arnold F, Kumar S. Angiogenesis induced by degradation products of hyaluronic acid. *Science*. 1985;228:1324–6.
46. Bhakta G, Rai B, Lim ZXH, Hui JH, Stein GS, van Wijnen AJ, Nurcombe V, Prestwich GD, Cool SM. Hyaluronic acid-based hydrogels functionalized with heparin that support controlled release of bioactive BMP-2. *Biomaterials*. 2012;33:6113–22.
47. Huang Y, Luo Q, Li X, Zhang F, Zhao S. Fabrication and in vitro evaluation of the collagen/hyaluronic acid PEM coating cross-linked with functionalized RGD peptide on titanium. *Acta Biomateriala*. 2012;8:866–77.
48. Chua P-H, Neoh K-G, Kang E-T, Wang W. Surface functionalization of titanium with hyaluronic acid/chitosan polyelectrolyte multilayers and RGD for promoting osteoblast functions and inhibiting bacterial adhesion. *Biomaterials*. 2008;29:1412–21.
49. Park JK, Shim JH, Kang KS, Yeom J, Jung HS, Kim JY, Lee KH, Kim TH, Kim SY, Cho DW, Hahn SK. Solid free-form fabrication of tissue engineering scaffolds with a poly(lactic-co-glycolic) grafted hyaluronic acid conjugate encapsulating an intact bone morphogenetic protein-2/poly(ethylene glycol) complex. *Adv Funct Mater*. 2011;21:2906–12.
50. Jiao Y, Liu Z, Shao X, Zhou C. Protein adsorption and cytocompatibility of poly(L-lactic acid) surfaces modified with biomacromolecules. *J Appl Polymer Sci*. 2012;125:E501–10.